

1 **Estimating fecundity and density dependence from mark-recapture data for**
2 **making population projections**

3 Bilgecan Şen¹*(Orcid ID: 0000-0002-7393-1805) and H. Reşit Akçakaya¹ (Orcid ID: 0000-0002-
4 8679-5929)

5 ¹Department of Ecology and Evolution, Stony Brook University, Stony Brook, NY, 11794,
6 U.S.A.

7 *Corresponding Author: bilgecan.sen@gmail.com

8

9 **Abstract**

10 Forecasting changes in size and distributions of populations is at the forefront of
11 ecological sciences in the 21st century. Such forecasts require robust estimators of fecundity,
12 survival and density-dependence. While survival estimation is the main focus of mark-recapture
13 modelling, fecundity and density dependence are rarely the subject of these models. Here, we
14 demonstrate that these parameters can be simultaneously estimated in a Bayesian framework
15 using only robust design mark-recapture data. Using simulated capture histories, we show that
16 this framework (which we named CJS-pop) can estimate vital rates and their density dependence
17 with little bias. When CJS-pop is applied to capture history data from Brown Creeper (*Certhia*
18 *americana*), it provides estimates of fecundity that is expected from the breeding biology of this
19 species. Finally, we illustrate that density dependence, even when estimated with uncertainty in
20 the CJS-pop framework, regularizes population dynamics and reduces the frequent population
21 extinctions and explosions observed under density-independent models. While CJS-pop as a
22 whole is a useful addition to the current mark-recapture modelling toolbox, we argue that the
23 independent components of this framework in estimating fecundity and density dependence can
24 be integrated to other CJS frameworks, potentially creating models capable of population
25 projections.

26

27 **Keywords:** CJS, CJS-pop, Fecundity, Mark-recapture, Population Models, Population
28 projections, Population Viability Analysis, Simulations

29

30 **Introduction**

31 Mark-recapture data analysis is a staple in population ecology for estimating survival,
32 abundance, and recruitment rates (Lebreton et al. 1992, Williams et al. 2002, Cooch and White
33 2016). More recently mark-recapture methods have been extended to work in parallel with
34 different types of data in frameworks such as integrated population models (IPMs; Schaub and
35 Abadi 2011) and to estimate dispersal and animal movement in spatial capture-recapture analysis
36 (Ergon and Gardner 2014, Schaub and Royle 2014). When considering the wide applicability of
37 mark-recapture methods for estimating parameters related to population dynamics, rarity of one
38 parameter in the mark-recapture literature stands out: fecundity as defined in a population
39 modelling setting, which is the number of juveniles per number of adults (for example, see Ryu
40 et al. 2016). If fecundity can be estimated from mark-recapture data, then this single data source
41 can be used on its own to parameterize stage-structured population models.
42 Ryu et al. (2016) provided a framework for estimation of fecundity and other necessary
43 population model parameters (stage-dependent survival, density dependence, and environmental
44 stochasticity) from robust design mark-recapture data. However, their framework is a mixture of
45 frequentist and Bayesian approaches of mark-recapture models and it requires multiple models to
46 be fit sequentially. As a result, Ryu et al. (2016)'s different model components do not inform one
47 another during estimation, which prevents making full use of the data at hand and propagating
48 uncertainty in a hierarchical manner. Here, we present an update on Ryu et al. (2016)'s
49 framework. We use both simulated and real data to show that; 1) fecundity can be estimated
50 alongside adult survival and capture probability in a single Bayesian framework using only
51 robust design mark-recapture data; 2) estimating fecundity reduces uncertainty in juvenile
52 survival estimates; and, 3) when these vital rates estimates are combined with density

53 dependence, resulting stage-structured population models are useful for calculating conservation-
54 relevant metrics.

55 **Material and Methods**

56 *Model specifications*

57 Two basic parameters are estimated in a standard CJS model (Cooch and White 2016):
58 survival and capture probability. Robust design mark-recapture data separates these two
59 processes to primary capture occasions (for example years), and secondary capture occasions
60 within primary occasions (for example months). Populations are assumed to be closed
61 (individuals don't die or leave the population) among secondary occasions within a primary
62 occasion. Capture probabilities are estimated for each secondary occasion, which can then be
63 used to estimate the population size for a given primary occasion. Populations are assumed to be
64 open among primary occasions, so individuals can leave the population or die. Survival is
65 estimated with information coming across primary occasions. Below, for simplicity in
66 presentation, we assume primary occasions are years and secondary occasions are months.

67 We denote $p_{x,k,t,h}$ as the monthly capture probability of a stage x individual at population
68 k , year t , and month h ; where, $x = 1,2,3 \dots, X$; $k = 1,2,3 \dots, K$; $t = 1,2,3 \dots, T$; and $h =$
69 $1,2,3 \dots, H$. We can use this monthly capture probability to calculate a yearly capture probability:

$$70 \quad P_{x,k,t} = 1 - \prod_{h=1}^H (1 - p_{x,k,t,h}) \quad (1)$$

71 Then, we can use the heuristic estimator of populations size with a correction for years
72 with no captures (Dail and Madsen 2011) to estimate the expected abundance of stage x
73 individuals at population k , year t :

$$74 \quad N_{x,k,t} = \frac{n_{x,k,t}}{P_{x,k,t}} + \frac{(1 - P_{x,k,t})}{P_{x,k,t}} \quad (2)$$

75 Where, $n_{x,k,t}$ is the number of captured stage x individuals in population k and year t . Using the
76 expected abundance time series of each population we calculate a density index:

$$77 \quad D_{k,t} = \frac{\sum_{x=1}^X N_{x,k,t}}{\frac{\sum_{t=1}^T \sum_{x=1}^X N_{x,k,t}}{T}} \quad (3)$$

78 where, $D_{k,t}$ is the density index at population k , year t . The numerator in equation 3 is the total
79 abundance of population k at year t across all stages, and denominator is the average expected
80 total abundance across T years. D is an index for the deviation of population abundance in a
81 given year from the long term average population abundance and it can be considered as a
82 relative population density. We use D as a covariate for estimating density dependence strength
83 of fecundity and survival.

84 All three parameters estimated by equations 1 to 3, namely, yearly capture probability,
85 expected abundance, and density index can be used to estimate fecundity and its density
86 dependence:

$$87 \quad \log(F_{k,t}) = \theta + \zeta \cdot D_{k,(t-1)} + \omega_{k,t} \quad (4a)$$

$$88 \quad \omega_{k,t} \sim \text{Normal}(0, \sigma_f^2) \quad (4b)$$

89 where, θ is the fecundity in log scale at 0 density; ζ is the change in fecundity in log scale with
90 one unit change in population density index; $\omega_{k,t}$ is the spatio-temporal random effect at
91 population k and time t ; and σ_f^2 is the spatio-temporal variance of fecundity at log scale. We link
92 the fecundity estimate to the data, which is the number of captured juveniles in a given year and
93 population, by using expected abundances for adults calculated in equation 2. Below we present
94 a simple case for two stages where $x = 1$ are juveniles and $x = 2$ are adults:

$$95 \quad N'_{1,k,t} = N_{2,k,t} \cdot F_{k,t} \quad (5a)$$

$$96 \quad n_{1,k,t} \sim \text{Poisson}(P_{1,k,t} \cdot N'_{1,k,t}) \quad (5b)$$

97 The expected number of juveniles is estimated twice in this framework: once as a derived
98 variable ($N_{1,k,t}$) using the heuristic population size estimator, and a second time ($N'_{1,k,t}$) as a
99 function of density and expected number of adults. We discuss this and our choice of Poisson
100 distribution in detail below.

101 So far, we have only used captured number of juveniles and adults as a data source.
102 However, this form of a capture history is not enough to estimate parameters used in the above 5
103 equations. So, we link these 5 equations with a more typical CJS model where survival and
104 capture probability are used to model capture histories of individuals:

$$105 \quad \text{logit}(\phi_{x,k,t}) = \alpha_x + \beta \cdot D_{k,t} + \epsilon_{k,t} \quad (6a)$$

$$106 \quad \epsilon_t \sim \text{Normal}(0, \sigma_s^2) \quad (6b)$$

107 where, $\phi_{x,k,t}$ is the apparent survival probability of a stage x individual at population k and year
108 t ; α_x is the survival probability of a stage x individual on logit scale at 0 density; β is the change
109 in survival in logit scale with one unit change in population density index; $\epsilon_{k,t}$ is the spatio-
110 temporal random effect at population k and time t ; and σ_f^2 is the spatio-temporal variance of
111 survival at logit scale.

112 Apparent survival changes the latent states of individuals in a population between time
113 steps, from t to $t + 1$; this latent state indicates whether an individual is alive and in the
114 population ($Z = 1$), or it is dead or left the population ($Z = 0$). The latent state of the i th
115 individual, then, is determined by its state at time t and its survival to time $t + 1$.

$$116 \quad Z_{i,(t+1)} \sim \text{Bernoulli}(Z_{i,t} \cdot \phi_{(S_{i,t}), (g_i), t}) \quad (7)$$

117 where, $\phi_{(S_{i,t}), (g_i), t}$ is the apparent survival probability at the breeding stage and population of the
118 i th individual from year t to $t + 1$; $S_{i,t}$ is a matrix indicating the breeding stage of the i th
119 individual in year t , and the vector g_i indicates the population that the i th individual is in. Latent

120 state, Z , also determines the potential capture of an individual; dead ones cannot be captured.

121 Hence, every element of the capture history, $y_{i,t,h}$ (1 if an individual is captured, 0 if it is not), is

122 a Bernoulli random variable with a monthly capture probability, $p_{(S_{i,t}),(g_i),t,h}$, conditional on the

123 individual being alive and in the population, $Z_{i,t}$.

$$124 \quad y_{i,t,h} \sim \text{Bernoulli}(Z_{i,t} \cdot p_{(S_{i,t}),(g_i),t,h}) \quad (8)$$

125 For simplicity in referring to this framework, we named it CJS-pop; pop extension comes from

126 the fact that it can estimate necessary parameters to build a stochastic and stage-based population

127 model: Fecundity, staged-based survival, density dependence, and process variance.

128 *Simulated data*

129 We simulated several sets of capture histories in order to test CJS-pop's ability to

130 correctly retrieve true parameter values, and to uncover any inherent biases, especially when

131 quantifying density dependence strength. We set up a simulation scheme where we explored the

132 effect of sample size on quantifying density dependence strength. We set the time series length to

133 17 years, which is the maximum time series length for Brown Creeper data set we are using (see

134 below). We simulated three cases with 1, 5, and 10 populations, and three carrying capacities

135 (which controls population size): 50, 100, 150. For each combination of the number of

136 populations and carrying capacity, we generated capture history data sets using weak, moderate

137 and strong density dependence on survival and fecundity, which created 27 separate simulation

138 sets. For each simulation set, we generated 56 capture history data sets and fitted CJS-pop to

139 each one. See Appendix S2 for more detailed discussion of the simulation framework and

140 Appendix S3 for its code.

141 *Empirical data: Brown Creeper*

142 We applied CJS-pop to Brown Creeper (*Certhia americana*) data obtained from the
143 Mapping Avian Productivity and Survivorship (MAPS) program. Brown Creeper is a widespread
144 North American songbird species. It is a resident, forest-dwelling bird in western U.S and along
145 the coastline to Alaska, in north-eastern U.S, and southern Canada. We treated each MAPS
146 location (a cluster of mist-netting and banding stations) of Brown Creeper to be a separate
147 population. We only included data from populations which were located in the contiguous U.S.,
148 and which have been monitored for at least 5 years. This resulted in a data set with 2931
149 individuals. We categorized any individual in its first year as a juvenile (MAPS age codes 2 and
150 4), and older individuals as adults (MAPS age codes 1, 5, 6, 7, and 8).

151 We made several adjustments and additions to basic CJS-pop framework presented above
152 when applying to Brown Creeper data. First, we accounted for potentially transient individuals in
153 the data set. In a CJS model, estimated survival rates are said to be “apparent” because the
154 estimated survival rate cannot distinguish between dead individuals and the ones that just left the
155 population. This can bias survival estimates to be lower than their true values. Accounting for
156 transients is a partial way to correct for this bias and it is a frequently used technique in CJS
157 literature (for example, Ahrestani et al. 2017).

158 Second, we used the priors and population modelling structure of CJS-pop to our
159 advantage to estimate a juvenile survival rate with less uncertainty. We use information from
160 adult survival and fecundity estimates, and the fact that they are density dependent, to estimate
161 juvenile survival:

$$162 \quad S_A + S_J \cdot F = 1 \quad (9)$$

163 where, S_A and S_J are survival rates of adults and juveniles at mean population size (when $D = 1$)
164 and F is the fecundity at mean population size. This equation states that population growth rate

165 (λ) is equal to 1 when population abundance is at its long-term average. Using this equation, we
166 would only need priors for adult survival and fecundity, and we can calculate juvenile survival
167 as:

$$168 \quad S_J = \frac{1 - S_A}{F} \quad (10)$$

169 Third, we used a zero-inflated Poisson for modelling fecundity in equation 5b because
170 there were several years and populations with no juvenile captures. Fourth, we did not use
171 populations and years with no adult captures when modelling fecundity. While we account for no
172 capture years in equation 2, we believe that limiting fecundity estimation to years with adult
173 captures provides a more robust estimate.

174 Fifth, we changed the spatio-temporal variance structure of survival to be only temporal.
175 Spatio-temporal variance structure in survival for Brown Creeper proved to be problematic
176 because it made convergence harder for multiple parameters while also reducing the effective
177 sample size of their MCMC chains. Lastly, we standardized the density index (D), calculated in
178 equation 3, to be 0 at mean population size. This allowed for faster convergence of the MCMC
179 chains in JAGS. See Appendix S2 for details on these adjustments to basic CJS-pop framework
180 and goodness-of-fit testing of CJS-pop .

181 We fit three different CJS-pop models to Brown Creeper data: 1) density dependent, 2)
182 density independent, and 3) Density dependent without the residency model.

183 *Population Projections*

184 We ran population projections using a stage-structured population model with
185 environmental and demographic stochasticity in both survival and fecundity. We parameterized
186 these population models with 3 different parameter sets:

187 1) True simulation parameters that we used to generate capture history data.

188 2) Parameter estimates from density-dependent and density-independent CJS-pop fit to
189 simulated data. At each replication we randomly selected the parameters of CJS-pop fit to
190 one of the 56 data sets with this population and carrying capacity combination. To further
191 incorporate parameter uncertainty, we randomly used at each replication the 2.5%, 50%,
192 or 97.5% percentiles of the selected parameters.

193 3) Parameter estimates obtained from CJS-pop fit to the Brown Creeper data. We employed
194 the full posterior distribution of the estimated parameters. At each iteration of the
195 projections, parameter estimates were randomly selected from the posterior distributions
196 of all parameters with respect to their correlation structure.

197 Using each of these sets of parameters, we ran single-population projections, with a
198 carrying capacity of 1000 and an initial population of 500 adults and 500 juveniles. We ran the
199 projections with 1000 replicates, and each replicate for 20 years. In order to incorporate
200 environmental stochasticity, at each iteration and at each year we generated random temporal
201 effects separately for survival and fecundity using σ_s^2 and σ_f^2 , respectively. We recorded the
202 minimum abundance of the population across 20 years for each iteration, and the distribution of
203 minimum abundance among iterations. The expected value of this distribution is called expected
204 minimum abundance (EMA) and it is a more informative metric than extinction risk, because the
205 latter often has a distribution restricted to near-zero or near-one values (McCarthy and
206 Thompson 2001).

207 *Software*

208 See appendix S2 for a list of R packages used in the analysis. We used JAGS as the
209 MCMC sampler when fitting CJS-pop to data. We ran the models with 4 chains, 50000
210 iterations, 20000 burn in, and a thinning rate of 10 for simulated data sets, and with 4 chains,

211 100000 iterations, 50000 burn in and a thinning rate of 20 for Brown Creeper data. We checked
212 convergence with R-hat values, and assumed chains were converged when \hat{R} was <1.05 . See
213 Appendix S4 for JAGS code of CJS-pop. Additionally, R and JAGS code of CJS-pop analysis,
214 example simulation data , and results of Brown Creeper analysis are accessible here:
215 <https://github.com/bilgecansen/CJS-pop>. The software source code has been archived and made
216 accessible in Zenodo (DOI: 10.5281/zenodo.3736702).

217 **Results**

218 *Simulations*

219 CJS-pop is able retrieve true parameter estimates without any apparent bias except for
220 density dependence (Figs. S1-6). DD strength is estimated with no bias when strength of DD
221 used to generate capture history data is moderate. Strong DD in data simulation leads to slight
222 underestimation of DD strength. There is, however, considerable overestimation of true DD
223 parameters when capture history simulation was carried out with weak DD strength (Fig. S1).

224 *Empirical Example: Brown Creeper*

225 We detected weak DD on survival ($\beta = -0.27$, Fig. 1a), and on fecundity ($\zeta = -0.13$,
226 Fig. 1b) for Brown Creeper. Process variance estimations are low for survival, and high for
227 fecundity, ($\sigma_s = 0.23$, $\sigma_f = 0.97$; Table S1). Survival at mean population size for adults and
228 juveniles were estimated at 0.42 and 0.31, respectively. Our estimate of fecundity at mean
229 population size was 1.94 (1.21 – 3.01) juveniles per adult (Table S1). In addition, Bayesian p-
230 values for both the survival and fecundity components indicated good model fits (0.24 and 0.50,
231 respectively).

232 *Projections*

233 Density-independent projections parameterized with CJS-pop fit to Brown Creeper data
234 lead to frequent population extinctions and explosions, which is apparent in the population
235 trajectory (Fig. 1c) and bi-modal distribution of minimum abundances (Fig. 2). Density
236 dependence in population models lead to more regularized projections in which population
237 extinctions and explosions are less frequent (Fig. 1c and Fig. 2). The distribution of minimum
238 abundances from density-dependent projections of Brown Creeper show a generally similar
239 pattern to projections parameterized with CJS-pop fit to simulated data irrespective of the DD
240 strength of capture history simulations (Fig. 2).

241 Projections made with population models that are parameterized with density-dependent
242 CJS-pop fit to simulated data are close to projections made with true simulation parameters,
243 especially when true simulation parameters included moderate or strong DD. This
244 correspondence demonstrates, in a biologically relevant context, the ability of CJS-pop to fit
245 realistic models to data (Figs 2c-d). In contrast, projections with density-independent CJS-pop
246 (Figs 2b-d), and with CJS-pop fit to simulated capture history data with weak DD (Fig. 2b) were
247 not close to projections with the true simulation models. Overestimation of DD strength in CJS-
248 pop fit to weak DD data also results in overestimation of projected minimum abundances.
249 Density-independent projections tends to result in frequent population extinctions or explosions
250 (Figs 2b-d).

251 **Discussion**

252 CJS-pop is ready to be applied to bird species captured in the MAPS program. It can be
253 extended to include weather, climate and other exogenous factors in addition to population
254 density. The true value of CJS-pop lies in its ability to use limited data to parameterize
255 population models that in turn can be used to predict changes in population sizes and

256 distributions. We believe this is especially important for developing countries that do not yet
257 have extensive bird banding and survey programs like MAPS and BBS. We don't, however,
258 think that whole CJS-pop framework needs to be used for the work we presented here to be
259 useful. Rather, we argue that the independent ideas explained in estimating fecundity, juvenile
260 survival and density dependence can be integrated to other CJS frameworks, potentially creating
261 models capable of population projections. Below we describe 4 of the main advances CJS-pop
262 provides to mark-recapture literature and discuss the trade-offs made when building the
263 framework.

264 *1 – Fecundity Estimation*

265 We estimated fecundity in the simulation data with no apparent bias (Figure S4). The
266 fecundity estimate for Brown Creeper ($F = 1.94$ (1.21 – 3.01); Table S1) is also biologically
267 realistic; Brown Creepers tend to have a single brood with a clutch size of 5 to 6 eggs in a
268 breeding season. The main contribution here is that every vital rate (including fecundity), capture
269 probabilities, and nuisance parameters were estimated simultaneously in a single model run. This
270 allows for propagation of uncertainty among these parameters but also makes it possible for
271 parameters that are estimated with less data (juvenile survival) to be informed by parameters
272 estimated with more data (fecundity and adult survival).

273 *2 – Juvenile Survival Estimation*

274 We detected no biases in juvenile survival estimates from CJS-pop in the simulation data
275 (Figure S2). Juvenile survival estimates of Brown Creeper were similar between a density-
276 dependent CJS-pop, and a CJS model that did not include fecundity or density dependence
277 estimation but accounted for “transient” juveniles that leave their population in their first year
278 (0.32 and 0.30, respectively). However, using information from fecundity and adult survival in

279 setting the prior for juvenile survival reduced the estimation uncertainty considerably in CJS-
280 pop. The 95% credible interval for juvenile survival in the CJS model is 0.08 – 0.71, while in
281 CJS-pop this interval is 0.19 – 0.48.

282 *3 – Density Dependence Strength Estimation*

283 Density dependence strength in mark-recapture studies is usually estimated using
284 abundance directly as a covariate (for example, Nater et al. 2018). This approach can become
285 problematic with more than one population, especially when each population has different
286 habitat characteristics and therefore can support different number of individuals. If the goal is to
287 estimate a species-specific density dependence strength that is applicable across all populations
288 of the species, abundance of each population in each time step should be standardized with a
289 proxy for how many individuals each population can support (e.g. carrying capacity). Here, we
290 made this standardization using long-term abundance average of each population (equation 3).
291 The density dependence strength we estimate is minimally biased for capture histories generated
292 by moderate and strong density dependence (Fig. S1). There is a more apparent bias when
293 capture histories are generated with weak density dependence (Fig. S1). However, the weak
294 density dependence strength we used does not constitute a biologically realistic scenario if we
295 consider the intrinsic growth rate associated with the density dependence strength from an
296 allometric standpoint (See Appendix S2 for discussion on this). Most importantly, density
297 dependence strength estimates of survival and fecundity are ready to be used for population
298 projections.

299 *4 – Population Projections*

300 Estimation of fecundity, juvenile survival, and density dependence strength makes it
301 possible to make population projections that are useful for conservation purposes. All of these

302 three vital rates and demographic parameters are required, in addition to what is estimated in
303 standard CJS models, to build a stage-structured population model. However, instead of
304 fecundity, a parameter called recruitment rate is frequently estimated from frameworks such as
305 IPM (for example, Ahrestani et al. 2017). This parameter cannot be used in stage-structured
306 population models because it combines information from both emigration rate and the number of
307 new-born individuals. Additionally, including only fecundity estimation in a CJS framework is
308 also not enough, because without density dependence, these population projections would not be
309 biologically meaningful. Population projections tend to explode in size or go extinct under
310 exponential growth when there is environmental stochasticity that is not regularized by density
311 dependence (Fig 1). The usefulness of this regularizing effect is also visible in the distribution of
312 minimum abundances from population projections. A density-independent model cannot capture
313 the minimum abundance distribution generated with a stochastic and density-dependent
314 simulation, even when density dependence is weak. (Fig 2).

315 *Trade-offs*

316 Using robust design mark-recapture data as the sole data set for the CJS-pop framework
317 requires several trade-offs. First, we estimate expected juvenile abundance twice (N_1 in equation
318 2 and N'_1 in equation 5a). If we only use N'_1 , JAGS will give an error regarding the circular
319 structure of the model because N'_1 would also have been used in the denominator of equation 3.
320 We see this as a minor issue because N'_1 is used in the estimation of fecundity and we showed
321 that fecundity can be estimated without bias in this structure (Figure S4).

322 Second, we estimate population sizes as expected values rather than random variables in
323 CJS-pop framework. Modelling population sizes as random variables either requires informative
324 priors on population sizes themselves or another data set, such as population counts, to make the

325 model more stable and allow convergence (this is essentially what IPMs do). Here, however, we
326 wanted to show that the vital rates necessary for population models can be estimated using only
327 mark-recapture data. Using expected abundance, while not ideal, ensures that this framework
328 requires only a single data source.

329 Third, we use a Poisson distribution instead of a binomial in equation 5b. Number of
330 captured juveniles cannot be higher than the actual number of juveniles; this relationship is
331 explicitly modelled as such with a binomial distribution. However, because we are using
332 expected abundances in CJS-pop, there could be instances when there are more captured
333 individuals than the expected abundance. Poisson distribution, by allowing such instances to
334 occur, increases model stability and eases convergence. Because Bayesian p-value for brown
335 creeper data is 0.5, we can say that this structure can represent the data well (Bayesian p-values
336 close to 0.5 indicate better fit; Kéry and Royle 2016). Last but not least, the framework we
337 present here is complex and in JAGS it takes for about 20 hours for Brown Creeper model to
338 converge.

339 **Acknowledgements**

340 We thank Kevin Shoemaker for valuable input. This study was initiated under funding
341 from the NASA Biodiversity Program (NNH10ZDA001N-BIOCLIM). We thank the many
342 volunteers who have contributed to the MAPS program and the Institute for Bird Populations for
343 development and active curation of the MAPS dataset.

344 **References**

345 Ahrestani, F. S., J. F. Saracco, J. R. Sauer, K. L. Pardieck, and J. A. Royle. 2017. An integrated
346 population model for bird monitoring in North America. *Ecological Applications* 27:916–
347 924.

- 348 Cooch, E. G., and G. C. White. 2016. Program Mark: A Gentle Introduction. 14th edition.
- 349 Dail, D., and L. Madsen. 2011. Models for Estimating Abundance from Repeated Counts of an
350 Open Metapopulation. *Biometrics* 67:577–587.
- 351 Ergon, T., and B. Gardner. 2014. Separating mortality and emigration: modelling space use,
352 dispersal and survival with robust-design spatial capture-recapture data. *Methods in*
353 *Ecology and Evolution* 5:1327–1336.
- 354 Kéry, M., and J. A. Royle. 2016. Applied hierarchical modeling in ecology: analysis of
355 distribution, abundance and species richness in R and BUGS. Elsevier/AP, Academic
356 Press is an imprint of Elsevier, Amsterdam ; Boston.
- 357 Lebreton, J.-D., K. P. Burnham, J. Clobert, and D. R. Anderson. 1992. Modeling Survival and
358 Testing Biological Hypotheses Using Marked Animals: A Unified Approach with Case
359 Studies. *Ecological Monographs* 62:67–118.
- 360 McCarthy, M. A., and C. Thompson. 2001. Expected minimum population size as a measure of
361 threat. *Animal Conservation* 4:351–355.
- 362 Ryu, H. Y., K. T. Shoemaker, É. Kneip, A. M. Pidgeon, P. J. Heglund, B. L. Bateman, W. E.
363 Thogmartin, and H. R. Akçakaya. 2016. Developing population models with data from
364 marked individuals. *Biological Conservation* 197:190–199.
- 365 Schaub, M., and F. Abadi. 2011. Integrated population models: a novel analysis framework for
366 deeper insights into population dynamics. *Journal of Ornithology* 152:227–237.
- 367 Schaub, M., and J. A. Royle. 2014. Estimating true instead of apparent survival using spatial
368 Cormack-Jolly-Seber models. *Methods in Ecology and Evolution* 5:1316–1326.
- 369 Williams, B. K., J. D. Nichols, and M. J. Conroy. 2002. Analysis and management of animal
370 populations: modeling, estimation, and decision making. Academic Press, San Diego.

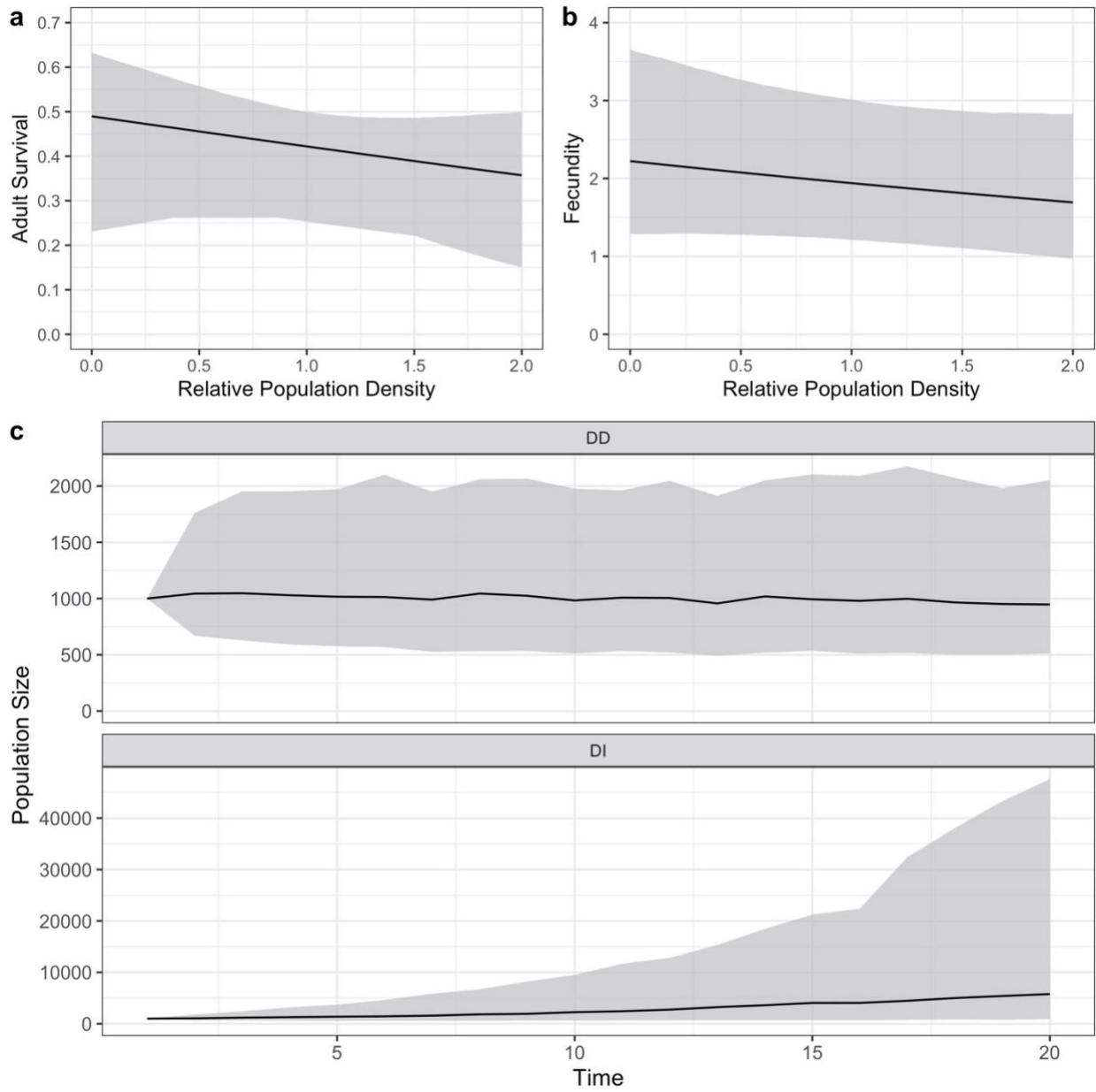
371 **Figure Legends**

372 **Figure 1:** a) Relationship between adult survival and relative population density (D) of
373 Brown Creeper as modeled by CJS-pop. b) Relationship between fecundity and relative
374 population density (D) of Brown Creeper as modeled by CJS-pop. c) Solid line indicates the
375 median trajectory of population size, across 12000 trajectories, of Brown Creeper projected by a
376 stage-structured population model that was parameterized with a Density-Dependent (DD) or
377 Density-Independent (DI) CJS pop. Shaded areas include 50% of the population trajectories.
378 Carrying capacity was set to 1000 in the DD projections. Note the difference in scale in
379 population size between DD and DI projections.

380 **Figure 2:** Distributions of minimum abundances resulting from population projections
381 made with stage-structured population models that were parameterized with CJS-pop fit to
382 Brown Creeper data (a), and with CJS-pop fit to simulation sets that was generated with different
383 density-dependence strengths (b,c,d). Light blue represents parameterizations of population
384 models with density-independent (DI) CJS-pop, orange represents density-dependent (DD) CJS-
385 pop, and green (TRUE) represents population models that was parameterized with original
386 simulation parameters that was used to generate capture history data. High probability density at
387 0 and 1000 indicates frequent population extinctions and explosions, respectively.

388

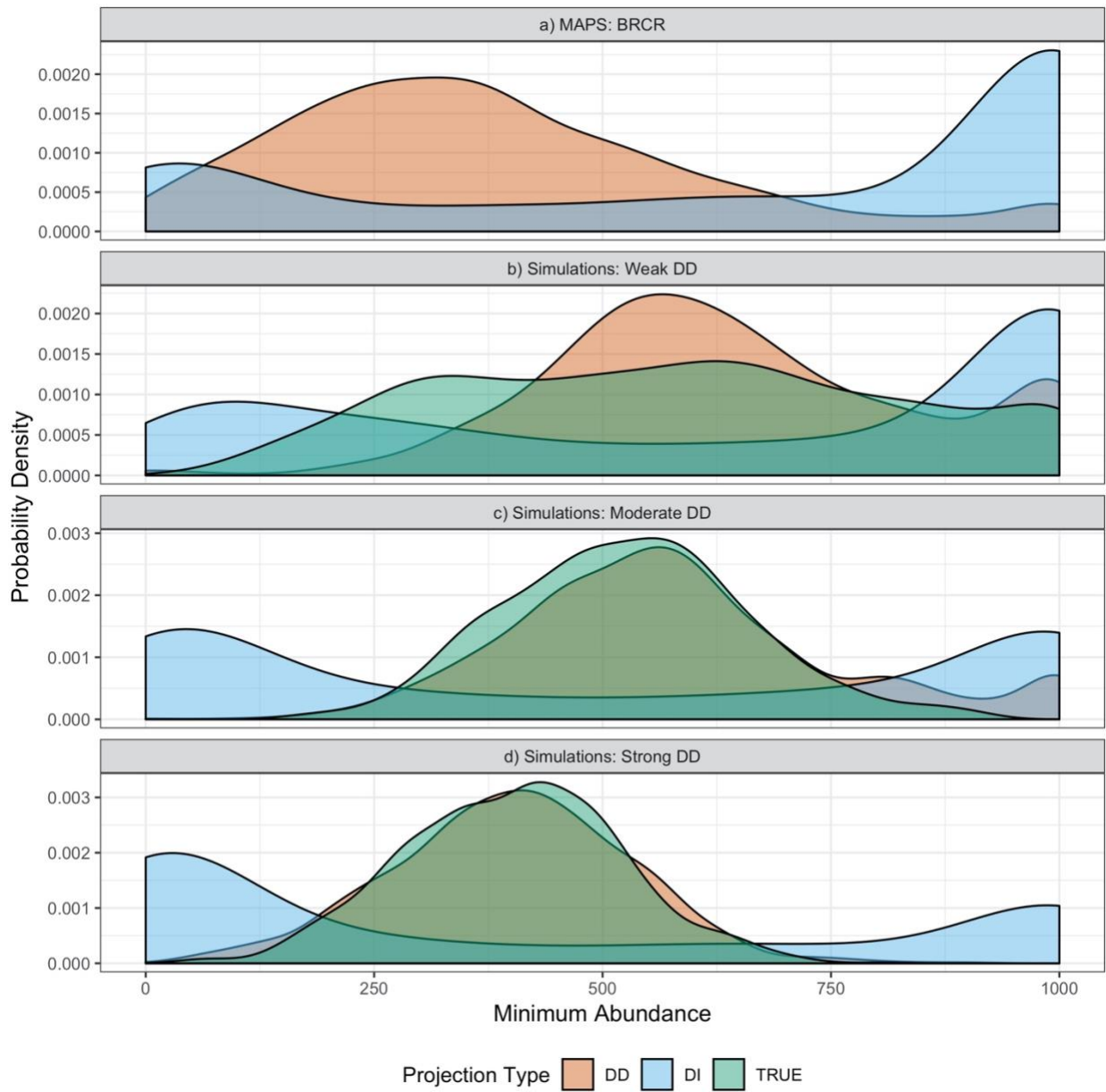
389 **Figure 1**



390

391

392 **Figure 2**



393